Daylight Transmittance Through Expanded Metal Shadings

Jose Miguel Rico-Martinez[1*], Marcin Brzezicki[2], Carlos Gabriel Ruiz-Mugica[1], Jakub Lech[2]

* Corresponding author
1 University of the Basque Country, School of Architecture, Spain, j.rico@ehu.eus
2 Wroclaw University of Science and Technology, Faculty of Architecture, Poland

Abstract

Due to the substantial need for energy efficiency, the daylight performance of building envelopes is a key issue in sustainable architecture. A frequently used shading system consists of static expanded metal meshes (EM). As a very prominent textural façade element, expanded metal is widely used as both a cladding and static shading device.

One initial aim is to provide a sufficient description of EM, including fabrication, possible usage, and overall properties. This includes a set of parameters needed to accurately control the complex geometry of EM. These parameters are also useful in getting reliable 3D computer models of EM.

The main objective of this paper is to assess, describe, and compare EM light transmittance performance for a shading device. Determining the influence of parameters such as geometry, colour, position, and direction of incoming light on the shading performance were specific objectives.

The research is based on BSDF simulations via Radiance (Ward, Mistrick, Lee, McNeil, & Jonsson, J., 2011) and experimental data provided at a previous laboratory stage.

The performance of various EM shading devices has been simulated and compared for a south-facing façade in Madrid for most characteristic times of the year: solstices and equinoxes, as well as midday transmittance throughout the year.

Keywords

Expanded metal, daylight transmittance, solar shading, bi-directional scattering distribution functions, angular selective shading systems

DOI 10.7480/jfde.2020.1.4698

1 INTRODUCTION

1.1 IMPORTANCE OF BUILDING ENVELOPES

The building envelope is the first protective barrier between the building and its surroundings, which gives it immense possibilities in contributing to the building's overall performance. One of the most notable is its influence on solar energy gains and overall daylight performance. Excessive heat gains constitute a serious problem in well-lit modern buildings, leading to higher energy usage, which is a serious economic and environmental issue. On the other hand, daylighting is a key issue in terms of visual comfort and energy savings through artificial lighting. Due to these circumstances, the daylight and thermal performance of building envelopes is a key issue in sustainable architecture (Littlefair, 2001).

1.2 DAYLIGHT IN BUILDINGS

Daylight is the combination of all direct and indirect sunlight throughout the day. Daylight creates the healthiest visual environment in buildings and provides an appropriate amount of illumination and all necessary spectral variety (including UV light). Scattered radiation (diffused daylight) does not cause major problems because it carries a relatively small amount of energy. In contrast, direct radiation (direct solar radiation) is associated with direct high-energy flux (approx. 1000 W per sq. m. of horizontal surface depending on the angle of incidence) (Begemann, van den Beld, & Tenner, 1997).

1.3 IMPORTANCE OF SHADING DEVICES

Buildings harvest daylight through glazed surfaces, which work as a single direction filter for infrared radiation, producing the so-called "greenhouse effect". The infrared range, from 780 to 1060 nm, involves heat transfer and causes temperature growth in rooms that too often are serviced by energy-consuming mechanical HVAC equipment in modern buildings, and characterised by a high percentage of transparent surfaces.

In the context of climate change and the energy use reduction requirements, shading systems are one of the most important issues in façade design. Shading devices protect the internal spaces from solar radiation, and – consequently – from temperature increase, but such devices should also allow for an adequate transmittance of daylight into the interior spaces of buildings. Besides those energy-related requirements, when designing continuous translucent layers, one must consider their permeability and optical performance for an adequate outward vision and privacy protection.

Another problem to address with shading devices is the appearance of discomfort glare, related to the presence in the visual field of excess luminance differences (Perry, 1990). In urban environments, façade glare affects visual comfort (discomfort glare) and influences the thermal load of other buildings (solar radiation from more than one source) (Brzezicki, 2012). In most buildings, glare protection is necessary to maintain proper visual comfort.

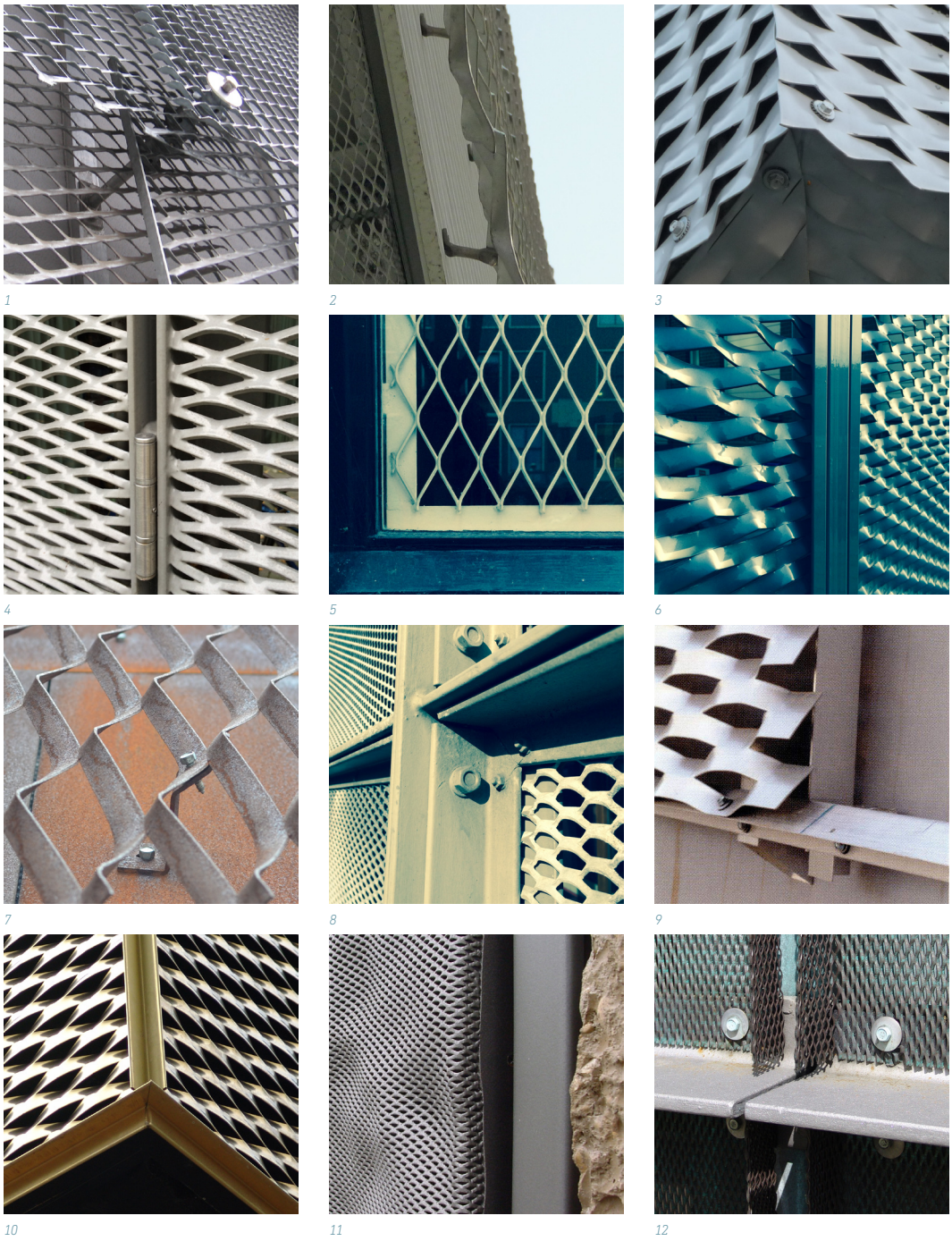

FIG. 1 Façade EM fixing solutions. Image 9 by Jesus Granada, first published in Tectonica n.22. Images 10,11,12 retrieved from https://www.flickr.com/photos/detlefschobert/ https://creativecommons.org/licenses/by-nd/2.0/

As well as with other materials or products, it is common practice to use EM as a sun control layer in façades, aiming to contribute both to thermal and visual comfort. If properly designed, EM meshes may allow daylight to pass through whenever necessary, as well as reducing cooling costs when used as sunshades. While highly effective in blocking direct sunlight, such systems must allow an adequate portion of the indirect, eye-friendly daylight through.

As EM is a metal product, one might be worried about the temperature it could reach under solar radiation and the subsequent radiative effect. As an initial benefit, EM will very often reflect radiation upwards, avoiding heat transfer to the ground. We have to consider the effect of colour and finish but, in general, EM shadings do not reach very high temperatures, probably due to the high proportion of voids and its easy ventilation.

Regarding wind resistance and acoustic behaviour, EM may need further specific studies relating to its behaviour to avoid excessive deformations and noisy turbulences. Those effects could be controlled by adjusting the geometry of the shading, size of the ventilated gap, and fixing system. In relation to the fixing, the nature of the fixing system must be addressed and many options are available, all of which must allow thermal expansion in order to avoid creaking (FIG 1.).

When calculating the wind load applied to the EM surface, if the voids are small and the percentage of voids is low (below around 20-30%), the whole surface of the EM is considered to bear the wind load, as if it were an opaque plate, disregarding the voids. This is due to the effect of the wind's sudden hit and the friction created when going through the mesh voids.

We could intuitively worry about wind whistling through the EM voids but, even if we cannot entirely disregard that option, the vast experience of installed EM façades allows that concern to be relaxed.

As EM is mostly installed as the outer layer of complex fenestration systems or ventilated façades, the maintenance and cleaning factor must be considered. Due to its geometry, EM can gather dust but as it is normally glossy or lacquered and the majority of the dust is washed off by rain, it does not require extraordinary maintenance measures. Besides, photocatalytic paints can be employed to create self-cleaning surfaces that avoid dirt and stains.

1.4 EXPANDED METAL FAÇADES

Angular selective shading systems such as Expanded Metal (EM) block direct sunlight and admit daylight within a specific range of incident solar angles (Fernandes, Lee, McNeil, Jonsson, Nouidui, Pang, & Hoffmann, 2015). EM presents a wide range of applications in architecture and the building industry but because of its prominent textural aspect, it is widely used as a façade element, both as the cladding of opaque surfaces and as a shading device. EM is a great fit for the needs of many contemporary architectural designers seeking continuous skins that envelop the whole building, blurring the difference between hollow and solid and providing a smooth light filter (FIG 2.)

Most other contemporary shading systems are constructed mainly for the momentary reduction of the energy flux, e.g. rollers, blinds, and shades, which are frequently integrated as a part of so-called adaptive façades (Loonen et al., 2015). Contrary to many complicated, mechanised shading systems, EM skins often define the appearance of the whole building, affecting both the building's physics (heat and light transmission) and the tectonics of the envelope.

As with façade louvres, EM meshes provide different shading patterns, depending on the angle of incoming sunlight. This allows for the passive regulation of the amount of transferred daylight throughout the year. However, the choice of EM variant will strongly affect the shading performance.

FIG. 2 Example of EM continuous skin. New Museum of Contemporary Art, New York. SANAA architecture office, 2007

One of the aims of this paper is to determine which aspects of EM design and manufacture should be considered in order to fit the requirements of each architectural design. The focus is on EM as a shading device, assessing its performance as an angular selective shading system and the influence of several parameters on the resulting daylight transmittance.

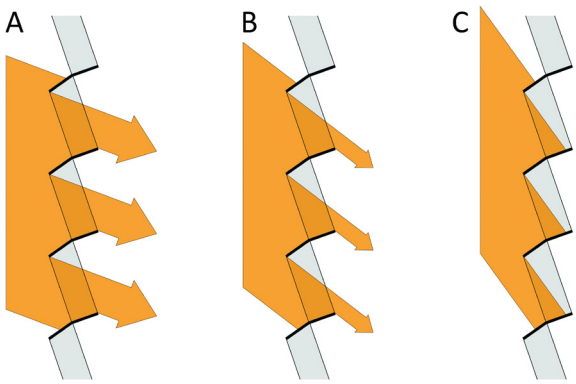

FIG. 3 EM as an angular selective shading

1.5 FABRICATION OF EXPANDED METAL

For an adequate understanding of the geometry of EM, which is necessary to build 3D models for simulation, an in-depth analysis of its shape and manufacturing process is needed.

EM is manufactured from metal sheets which have thicknesses usually ranging from 0.4mm to 6 mm. The manufacture consists of shearing and stretching operations in a press, leaving voids surrounded by the stretched strands of metal. Aluminium, mild steel, galvanised steel, stainless steel, copper, brass, nickel, titanium, platinum, zinc, silver, and gold are possible materials for manufacture, but companies produce 80 - 90 % in steel. Following the mechanical manufacturing operation, the resulting mesh can be coated by lacquer finishes or by galvanisation.

FIG 4. shows a sketch of the described mechanical operation. The metal sheet advances on a conveyor belt towards the press. A vertical movement of the blade (move 1) makes a row of cuts perpendicular to the advancing movement of the sheet (move 3) and simultaneously distorts the part of the sheet that has advanced beyond the cutting-line, pushing it downwards. After this first cut-and-push operation, the blade rises and moves a certain horizontal distance (move 2) perpendicular to the advancing movement of the sheet. This way, two rows of cuts end up displaced one from each other in a zigzag pattern.

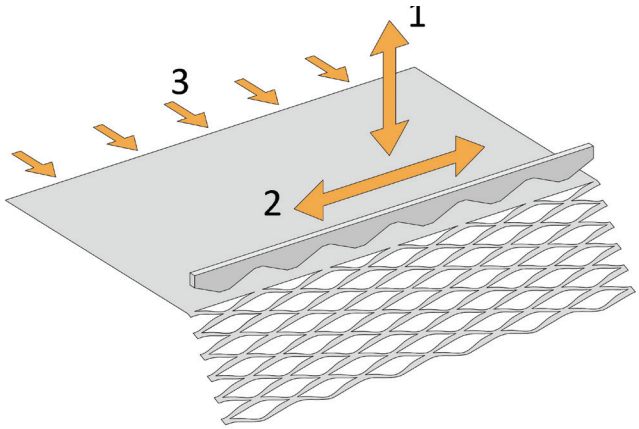

FIG. 4 The three manufacture movements

There are several kinds of EM, depending on the form and magnitude of the movements of the blade and the consequent shape of the holes. The simplest and most common type has rhomboid holes, usually known as rhombus-shaped or diamond-shaped; this will be the object of our research.

EM offers some advantages compared to other techniques: it is formed from a single piece of metal; no welding or weaving the metal is needed; neither joints nor welded knots are created and therefore there is less risk of rupture. Compared to other translucent metal screens such as perforated metal or woven metal fabrics, EM can offer greater flexural stiffness because the manufactured mesh has a larger overall thickness and therefore a better moment of inertia than the initial metal sheet. This feature of EM makes it very appropriate for installation in façades, as wind pressure is acting on them.

EM can be used for outdoor installation with different thicknesses of the departing metal coil, depending on the metal used, the geometry of the mesh, its finish and the distance between fixing points. Each mesh has a different moment of inertia (flexural strength) depending on the overall thickness the mesh achieves after expansion, which ultimately depends on the height of the peaks of each rhombus and the strand width.

In practice, designers and manufacturers do not perform such analysis to achieve a precise design, and the vast accumulated experience leads to using metal plates of minimum 2-3 mm in aluminium (depending on the alloy and geometry) and 1.5-2 mm in pre-galvanised steel. Even if these two materials are a good choice against corrosion, they are usually coated with powder paint in the case of pre-galvanised steel and powder paint or anodising in the case of aluminum. It is worth considering that for thicknesses of pre-galvanised steel lower than 2mm, the edges that become unprotected after the cutting operation are covered by the remaining rusting residues of zinc, as a kind of self-protection.

In terms of regulation, there is no specific regulation for EM. In Europe, projects have to conform to Eurocodes regarding loads and, being conservative, the aforementioned thicknesses cover almost all cases. In the USA, there is a more conservative approach and it is usual to prescribe larger thicknesses because of civil liability concerns.

1.6 EXPANDED METAL GEOMETRY

The geometry of a rhombus-shaped EM mesh can be described using some parameters of the mesh and press-machine shown in FIG 5: Long way mesh (LW), short way mesh (SW), strand thickness (e), strand width (w), intercut (i), cut width (c), blade bevel width (b), and blade thickness (t). The elongated metal strips that form the mesh are called strands and the joining area of four strands is called *knuckle* or *bond*.

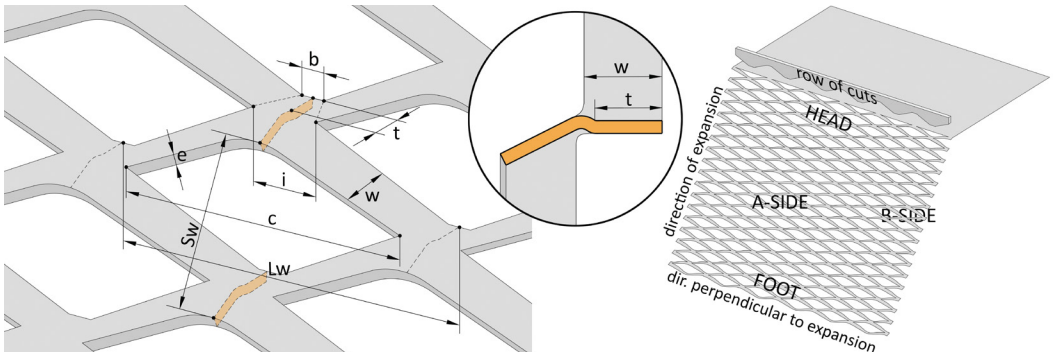

FIG. 5 A: Geometrical parameters of an EM mesh. B: Position and side-references related to the manufacturing process

Taking into consideration the available geometrical parameters and materials, one can get a countless number of different types of possible EM manufactures.

The use of EM as the external envelope in building façades has become more and more common in recent decades and designers often choose meshes with bigger nerves and holes than in other applications. Many manufacturing companies have a range of products under an architectural or decorative heading, including a wider variety of colours and sizes.

Analysis of shadow patterns cast by EM shows that those meshes with large openings are not the best option for façades of workspaces as the projected shadow patterns would involve glare and visual problems. Anyway, indoor diffusing technical sunscreens are usually used to solve this issue. Designers do install EM normally in façades of spaces used for sport, leisure, culture, commercial or circulation. EM with finer nerves offers more uniform shading patterns, but also can provide less shading performance, and therefore may be less effective in reducing overheating in the space.

EM elements shade rooms, but also act the other way round as a selective filter, that partially blocks selected parts of the field of vision. Due to EM geometry, this outward vision depends on the angle between the line of vision and the EM panel. If the observer's line of vision is perpendicular to the EM plane, the visual permeability of EM will depend on the EM mesh parameters, mainly strand width, as shown in FIG 7. With the change of this angle the permeability will show the angular selective performance of EM, meaning basically that at certain angles EM visibility will be minimised (with the observer looking down), while at the other, outward vision will be entirely blocked (with the observer looking at the steep angle up). This issue of the visibility and perforated envelope is addressed in detail in a recent PhD thesis (Alatawneh, Rosario, Germanà, & Reffat, 2016).

2 METHODOLOGY

Chronologically, our conducted research is divided into the following stages:

- Choice of assessment method and parameters
- Preparation of 3-d models
- Radiance simulation
- Verification of BSDF results comparing with previous lab results
- Extraction and processing of BSDF data
- Result interpretation

2.1 MEASUREMENT METHOD

The most popular measure of daylight performance in buildings was the daylight factor (light inside space/light outside the space ratio) (Robbins, 1985). This is quite easily measurable and provides the daylighting value at a point on a horizontal work plane in the room but does not provide any information about the direction of incident light and its distribution after transmission. Daylight factor provides information about daylight in the case of evenly overcast sky, and therefore is not suitable to assess the momentary values of the illuminance in the room resulting from direct sunlight, changing continuously according to the sun path. The development of simulation software demonstrated that more complex concepts than daylight factors were necessary.

Daylight Transmittance is the ratio of the amount of light transmitted through a window divided by the amount of light incident on its outside surface.

With Hemispherical Transmittance and Reflectance, one gets an overall amount of light going through, and reflected from the material but those magnitudes do not tell us anything about light distribution after transmission or reflection. Bidirectional Scattering Distribution Functions (Ward, Mistrick, Lee, McNeil, & Jonsson, 2011) describe the behaviour of light when reaching an opaque or translucent surface, for various angles of incidence of light on that surface and various angles of reflected and transmitted light. Based on Nicodemus and Klems' works (Klems, 1994; Nicodemus, 1965) a method was created to compile the directional behaviour of fenestration systems as regards reflection and transmission of radiation in a matrix. The BSDF of a surface is a four-dimensional function that, in simple words, describes how the surface scatters radiation. In the strict sense, the data that will be managed will be the BTDF (Bidirectional Transmittance Distribution Function) as the purpose of our work is the assessment of the daylight transmittance of EM.

Even if BSDF has the potential to provide detailed information about the way a material scatters light, the focus in this paper is not to assess the distribution of scattered light, but to assess how the overall transmittance or hemispherical transmittance is affected by different parameters of EM.

2.2 SOFTWARE AND SIMULATION RESULTS VERIFICATION

The 3-D models used for simulation were generated by a custom-made Grasshopper (for Rhino) algorithm, based on the parameters described in FIG 5. To ensure the high accuracy of the generated models, some of them were compared with 3-d scans of their real-life counterparts, which led to further modifications in the algorithm (Rico-Martinez, 2015).

The BSDF simulations were run via the *genBSDF* command from Radiance software (McNeil, Jonsson, & Appelfeld, 2011). This provided us with a large-size data pool, from which the data required to assess real-life daylighting situations could be later extracted.

Values from Klems-based BSDF were verified by comparison with experimental data provided at a previous laboratory assessment campaign in the context of a PhD research (Rico-Martinez, 2015). One of the main limitations of the lab setup (FIG 11.) used to measure the daylight transmittance of physical samples was the ability to measure the illuminance only in a small area and provide only specular transmittances. It was a sufficient method for measuring the direct specular transmittance, which is normally about 99% of the total, as it provided a uniformly lit constant light pattern, helped by a diffuser. However, this is a disadvantage when the indirect transmittance constitutes a more significant fraction of overall transmittance; e.g. meshes with bigger openings or extreme angles of incoming light directions, nearly parallel to the mesh plane, where interior reflections and consequent scattered light can be of greater importance.

The previous limitations are not an issue in the case of BSDF simulation, as it analyses the full spectrum of angles for both income and outcome directions.

2.3 PERFORMANCE COMPARISON - CHOSEN INPUT PARAMETERS

Based on the previous lab results and visual observation of various mesh variants, it was determined that the SW/w ratio or *EM opening ratio* (short way of mesh/strand width), could be used as a depictive feature of EM geometry (FIG 6.).

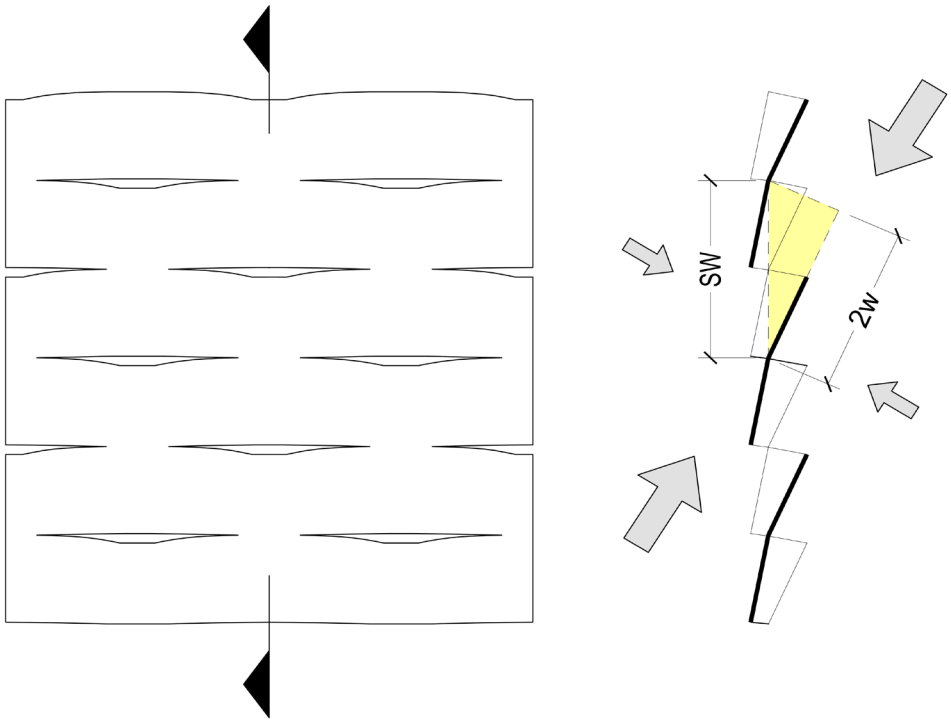

FIG. 6 Transmittance through a mesh with a low opening ratio (SW/w) ratio

For this paper, strand width (w) will be the main varying parameter, as it directly influences the SW/w ratio and the surface of the opaque areas of an EM mesh. All the geometrical parameters that do not rely on strand width will be kept constant, in order to allow for a reliable comparison.

2.3.1 Mesh type, time, position and localisation

In the presented paper, daylight transmittance through diamond-shaped EM shading devices is assessed in a vertical position with face "A" (FIG 5) on a south-facing façade, located in Madrid at most characteristic times of the year: solstices and equinoxes, as well as midday throughout the year.

- Mesh type – EM with diamond-shaped holes. Different variants of the most common EM type in building envelopes are simulated and compared.
- Position – south façade. Mesh placed in the typical, vertical position that provides the best shading performance. The south-facing position was chosen because it provides the longest sun exposure (north hemisphere).

— Location – Madrid. (40° 25' N 3° 42' W). Madrid has a warm climate (annual temperature during the day: 19.9 °C/67.8 °F) and one of the longest durations of sunshine in Europe (2769 hours per year). Latitude provides a variety of measurable sun angles throughout the whole year.

2.3.2 Mesh variants chosen for simulation. Strand width variation

A set of six modelled meshes (FIG 8.) was prepared, with only one differing parameter: strand width (w).

The following three EM parameters: SW, d, and w, form a right-angled triangle. Consequently, keeping the dimension of the Short Way (SW) constant, any variation in strand width (w) results in a change in the manufacture's blade descent (d).

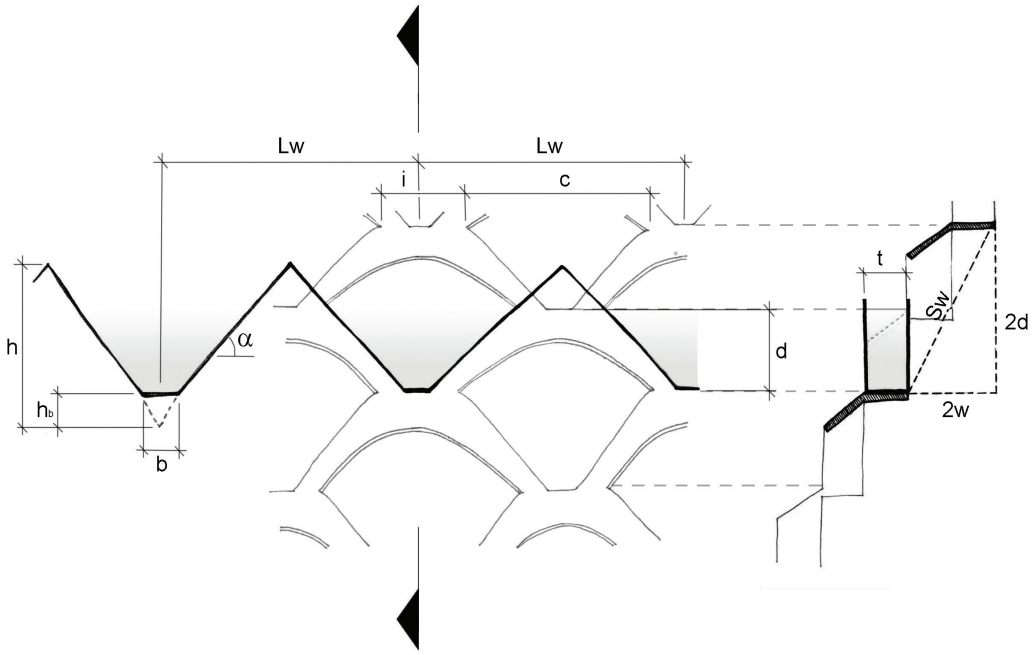

FIG. 7 Parameters of an EM mesh. Long way of mesh (LW), short way of mesh (SW), intercut (i), cut width (c), blade bevel width (b), blade thickness (t), blade descent (d), blade tooth's height (h), bevel's height (hb), blade's slope (α)

Besides, the slope of the blade (α) also varies if the strand width (w) is changed and all other parameters are fixed.

The limits for the strand width (w) are:

A w>e. This is an approximate limit due to fabrication conditions.

B w<SW/2. Elsewhere, the blade does not descend; therefore, the expansion of the mesh does not occur.

The following table shows the parameters of the EM meshes assessed.

TABLE 1 Values of the geometrical parameters defining the assessed EM meshes

LW	SW	W	E	B	I	D	A	SW/W
200	73	6	1	7	33	36.00	24.23	12.17
200	73	12	1	7	33	34.47	23.31	6.09
200	73	18	1	7	33	31.75	21.65	4.06
200	73	24	1	7	33	27.50	18.97	3.05
200	73	30	1	7	33	20.79	14.57	2.44
200	73	35	1	7	33	10.36	7.38	2.09

Obviously, the increase of strand width (w) is inversely proportional to the one of the EM opening ratio (SW/w). This way, the thinner the EM strands, the wider the mesh expansion and, therefore, the openings are larger. Logically, high values of opening ratio should lead to high values of transmittance.

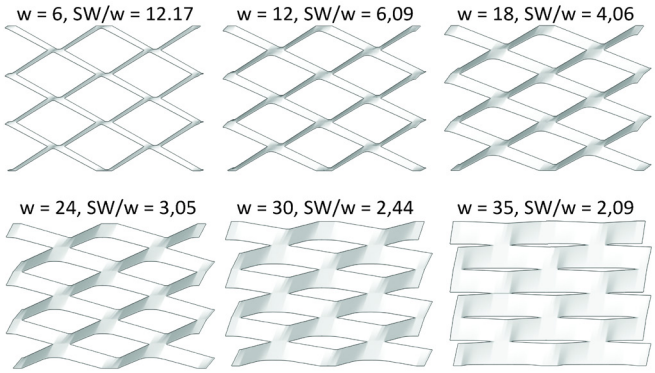

FIG. 8 Front views of EM geometrical variants used for the assessment

2.3.3 Mesh variants chosen for simulation. Colour variation

The impact of colour will also be considered, assessing each mesh in three colours: black, grey, and white. The same colour and reflectance values will be used, as in the previous lab assessments with real meshes. For those lacquers, the following reflectance data through spectrophotometry was obtained:

TABLE 2 Total reflectance and reflectance without specular component of analysed EM meshes finishing lacquers (measured with spectrophotometer)

COLOUR	REFLECTANCE (%)		REFLECTANCE WITHOUT SPECULAR COMPONENT (%)	
White	84.1	+/- 0.3	80.9	+/- 0.6
Grey	43.1	+/- 0.2	39.5	+/- 0.3
Black	4.4	+/- 0.1	4.2	+/- 0.1

2.4 EXTRACTION OF BSDF DATA FOR REAL DAYLIGHT SITUATIONS.

2.4.1 Data extraction

In the case of this study, the focus is on the overall percentage of transmitted rays, i.e. hemispherical transmittance (specular + scattered), which will be later referred to as *transmittance*. This paper does not differentiate scattered from specular light, as specular transmittance through EM is much higher than scattered, and hemispherical data is needed to compare the overall behaviour of different meshes at different moments.

Even if BSDF has the capacity to provide directional information about transmittance, for the aim of this paper, comparing overall data in a simplified manner is needed. Anyway, our previous experience tells us that, except for incoming light directions nearly tangential to the mesh plane, the majority of the light through the wide variety of EM meshes assessed in our computer BSDF assessment consists of specular transmittance. The rest of the values, surrounding this peak, refer to scattered transmission, which comes from the reflection of light in the mesh's strands. Among these values, we could observe some of the most significant reflection directions where transmittance values are higher. Anyway, the specular transmission takes more than 90% of the hemispherical transmission (Rico-Martinez, 2015).

In fact, we had to use a logarithmic scale (base 10) for graphs representing transmittance values in different directions because the value of the transmittance (ratio of incoming to outgoing light) in the specular direction was often bigger than 1% and lower than 0.01% for the scattering directions. The use of the logarithms of the transmittance values rather than the actual transmittance values reduces a wide range to a more manageable size. Moreover, human senses and perception are supposed to work in a logarithmic way (hearing, sight, etc.).

As the shading performance of EM is being assessed, direct sun radiation in real-life cases is assumed, i.e. one main incoming light direction.

One of the challenges was that the data about incoming light directions from BSDF simulation is related to each Klems patch and does not correspond precisely to the directions of sunlight obtained for real situations (described by linear sun paths, the daily arc-like path that the sun appears to follow across the sky). It was necessary to properly adapt the BSDF simulation data to assess the mesh's real-life performance.

BSDF data follow a coordinate system, called the Klems angle basis, which was designed specifically to simplify a matrix multiplication to model multi-layer window heat gains. The Klems angle basis has 145 input and output directions. Each direction is related to a patch of the hemisphere and all the patches have roughly the same cosine-weighted solid angle. Consistency in the cosine-weighted solid angle ensures that the contribution to hemispherical transmittance is roughly the same for all patches (McNeil, Jonsson, Appelfeld, Ward, & Lee, 2013).

Extracting the useful data meant selecting the Klems patches involving the desired sun directions. This resulted in obtaining patterns of Klems patches (FIG. 8) resembling a pixelated version of the actual sun path (FIG 9. S.P.). As the selected sun paths do not necessarily cross the centres of the patches, in some cases, it has been necessary to obtain transmittance values for additional regions (FIG 9. B) in order to calculate arithmetic averages of transmittance values of the involved patches.

The following software has been used to obtain the sun paths: Ladybug Tools (Grasshopper plugin for Rhino 5) (Sadeghipour Roudsari n.d.) and Curic Sun plugin for Sketch-Up (Curic Studio n.d.).

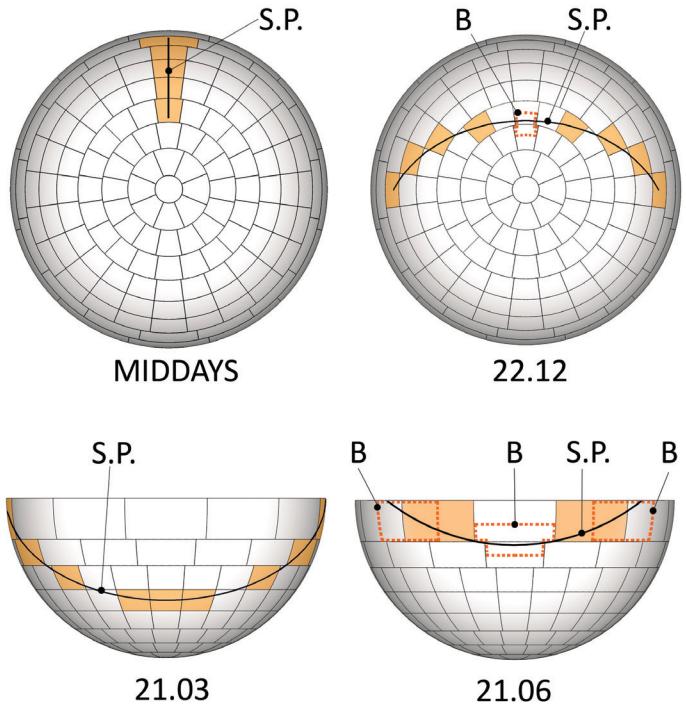

FIG. 9 Examples of sun paths (S.P.) related to patch sets on the Klems dome. Midday, winter solstice (22.12), equinox (21.03) and summer solstice (21.06)

Procedure for transmittance assessment throughout a day

To obtain the data about transmittance through a particular day, the geolocation and position of the mesh, as well as the date, were first specified. One could then obtain the corresponding sun-path, which describes the consecutive sun positions throughout that day.

Each Klems patch was described with the direction defined by its geometrical centre (FIG 10. C) and the closest point from each patch centre on the sun path was found. That point represents a sun position related to a daytime-value (FIG 10. C'). As a side effect, the method resulted in atypical values of daytime slots in the abscissa (e.g. 7:12, 9:36, 14:24, and 16:48) but related to quite precise transmittance values.

Procedure for transmittance throughout a year

Likewise, midday transmittance values through the year (FIG 9. midday) were obtained considering the 365 days of the year at 12:00, picking the incident patches with centres on that longitude fragment, finding the sun positions that match with the patch centres and finally matching the date values to those points. Again, this resulted in atypical values of date slots in the abscissa (e.g. 21th January, 23rd February, 21st March, 17th April, and 24th May) but related to precise transmittance values.

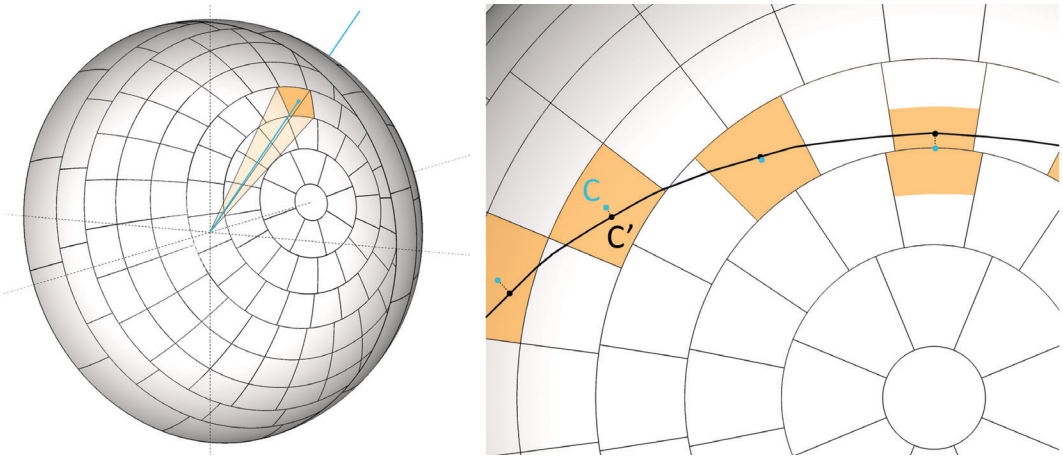

FIG. 10 Geometrical centre of a single patch. [C] patch centre [C'] the closest point on the sun path

3 PREVIOUS RESEARCH AND EXPERIMENT

3.1 COMPARISON OF LAB DATA AND BSDF SIMULATION RESULTS

In the aforementioned research (Rico-Martinez, 2015), the BSDF data running simulations were validated for models that were previously assessed in the laboratory (FIG. 11) with real samples. Overall, apart from those directions with the most extreme angles, the BSDF simulation results didn't show much deviation from lab results with an average of 4.96% (considering all incident light angles, including the most extreme, tangential ones, the overall average of deviation was 10.17%).

For those specific extreme angles, transmittance values were significantly higher for the computer simulation data and it was concluded that the physical model readings were significantly lower than the real ones, due to the lab setup limitations. However, the BSDF data obtained were consistent, as has been proven by the work and practice of many authors. (McNeil, Jonsson, Appelfeld, Ward, & Lee, 2013) (De Michele, Loonen, Saini, Favoino, Avesani, Papaiz & Gasparella, 2018) (Saini, Loonen, & Hensen, 2018).

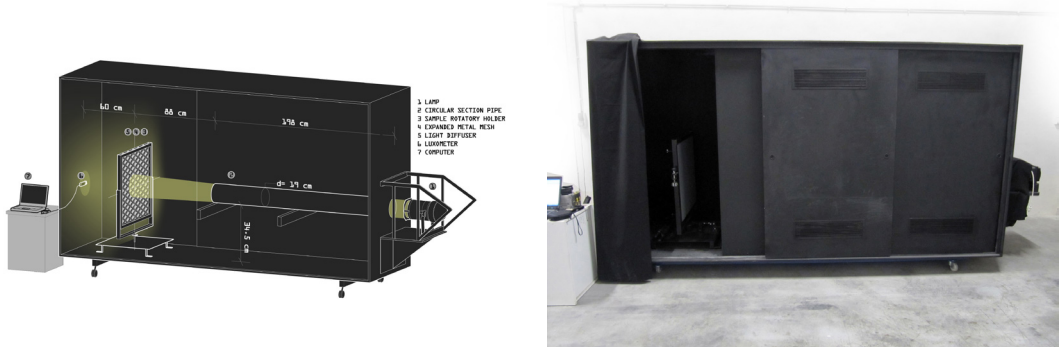

a b

FIG. 11 [a] Scheme of Lab assessment setup [B] Picture of the setup

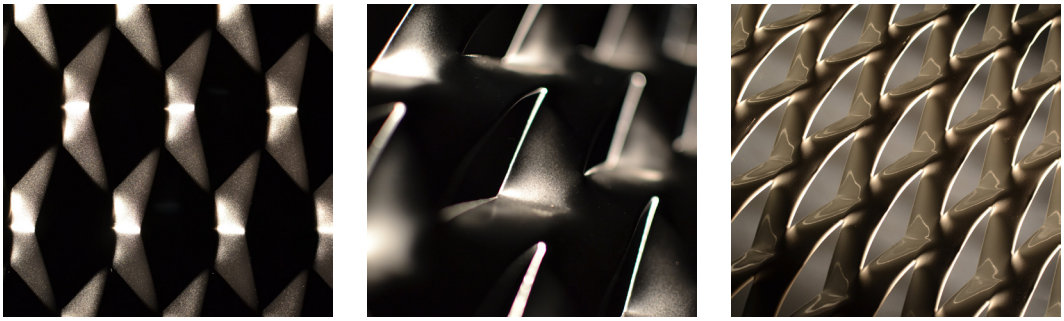

FIG. 12 Lit EM meshes in the lab setup

4 RESULTS AND DISCUSSION

In the following sections, the data obtained through simulation is presented in the form of graphs for the aforementioned colours, dates, and six types of EM.

The first three sets of graphs deal with the transmittance through the day.

The subsequent set of graphs shows midday transmittance values throughout the year.

Then, two sets of graphs are included using the same data but rearranging it. This way the influence of strand width on daily transmittance is described, by times of the day, and the influence of strand width on midday transmittance, by dates.

This section finishes with a table that quantifies the influence of colour on transmittance.

It is worth remembering that the following charts offer hemispherical transmittance data, the sum of scattered and specular light transmittance. For each incoming light direction, we obtain a unique value of transmittance expressed as a percentage (percentage of the incoming light transmitted through the EM mesh).

Likewise, it is important to remember that only direct incoming light is considered, i.e. clear sky conditions, which are the raison d'être of solar shadings.

4.1 TRANSMITTANCE VALUES THROUGH THE DAY BY STRAND WIDTH FOR SPECIFIC COLORS AND DATES

4.1.1 Winter Solstice

Besides being the shortest day of the year, the lowest solar angles are characteristic of the winter solstice (FIG 13.). In such conditions, all simulated variants of EM seem to function as expected, with transmittance values dropping very slightly towards midday as solar height increases.
The only visible divergence seems to be a slight increase in transmittance around midday for the 12 mm strand width mesh (w=12mm). This can be due to the complex geometry of EM or to method inaccuracies like the ones described in 2.4.1 about the relation between the real sun path and the available light directions from the Klems basis.

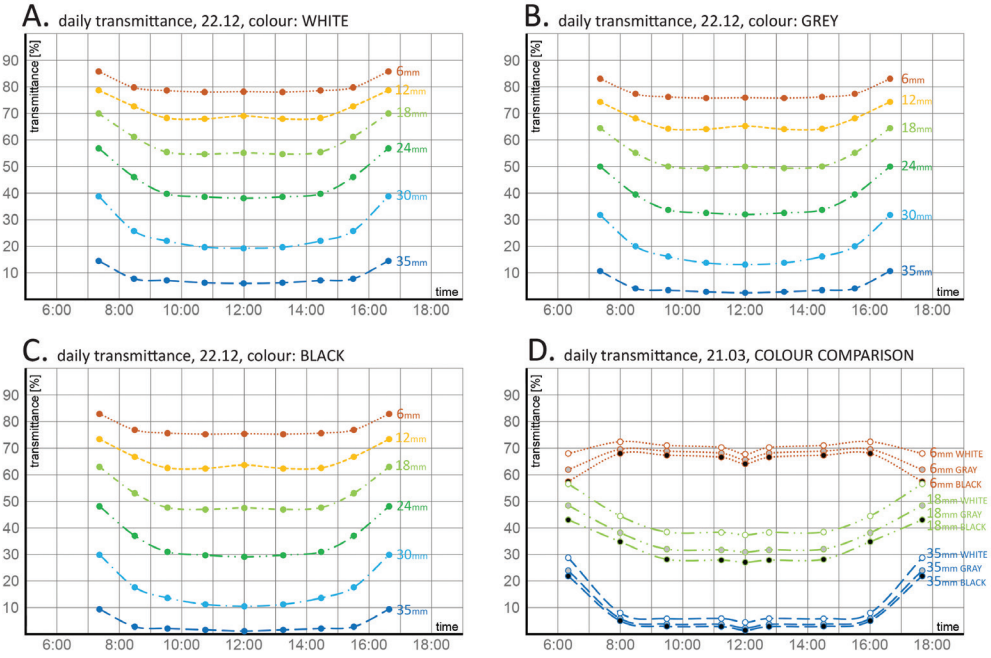

FIG. 13 Transmittance data throughout the day for the winter solstice. Each curve corresponds to a given strand-width, w (mm). The first three graphs correspond to each colour: white, grey and black. The fourth graph shows the superposition of curves for the three colours and three strand-widths: 6, 24 and 35mm

It also worth noticing, that for most of the day, the transmittance curve of w=35mm mesh seems to run almost flat, with transmittance below 10% for white and 4% for black finish.

In any case, all the curves present low amplitudes and moderate variations throughout the day due to colour. Almost all the curves show an upwards concavity with maximum values at dawn/dusk and minimum at noon. The 24 mm and 25 mm strand width meshes show the biggest amplitudes.

Bigger increases regarding noon values appear for the intermediate meshes (w=24 mm, w=30mm). Those increases approach 20 percent points, whereas for the extreme meshes, with maximum and minimum translucency (w=6 mm and w=35mm), those differences drop to around eight percent points.

In general, there is a great transmittance increase from w=35mm to w=6mm (around 70-75 percent points), which shows that the effect of modifying the strand width in winter is substantial.

The transmittance increase due to the colour of the mesh is greater for the intermediate meshes (w=24 mm, w=30mm), which present an increase of 10 percent points at 12:00 when it changes from black to white. The difference between black and grey is low, almost half of the difference between grey and white.

4.1.2 Spring/Autumn Equinox

At the equinox (FIG 14.), EM meshes with strand width w=18mm and higher seem to perform as expected with lowest transmittance values at midday, and rise towards dawn/dusk. It is also worth noticing that for a significant portion of the day (even around 8:30-15:30 for 35mm mesh) transmittance values seem to remain roughly constant.

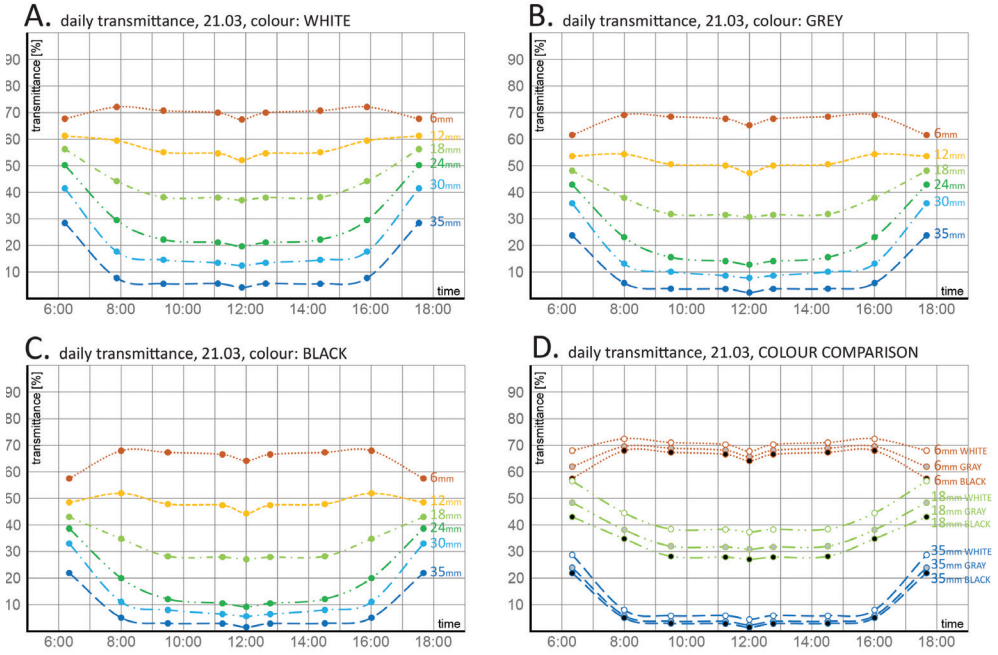

FIG. 14 Transmittance data through the day for spring/autumn equinox (21 March / 22 September). Each curve corresponds to a given strand-width, w (mm). The first three graphs correspond to each colour: white, grey and black. The fourth graph shows the superposition of curves for the three colours and three strand-widths: 6, 24, and 35mm

12mm mesh seems to maintain quite similar values throughout the day.

With the exception of the 6 mm strand width mesh, again the curves show upwards concavities but with higher differences between dawn/dusk and midday than in the winter (FIG 13.) and summer solstices (FIG 15.). The maximum amplitude is about 30 percent points. This agrees with the sun path, as it is rising towards midday and the EM strands are blocking a greater amount of rays. However, when the strand width value is low, those differences are blurred.

If one pays attention to the effect of colour, it can be noticed that it is more noticeable at dawn/dusk with a variation of around 10 percent points from black to white. This is more evident for the intermediate meshes (w=12 mm, w=18 mm, w=24 mm) and gets lower as strand with increases. For w=35 mm the colour effect is around three percent points at midday and seven points at dawn/dusk.

For the rest of the daytime, in general, the effect of colour is less evident.

No noticeable difference arises in the jumps from black to grey and from grey to white.

4.1.3 Summer Solstice

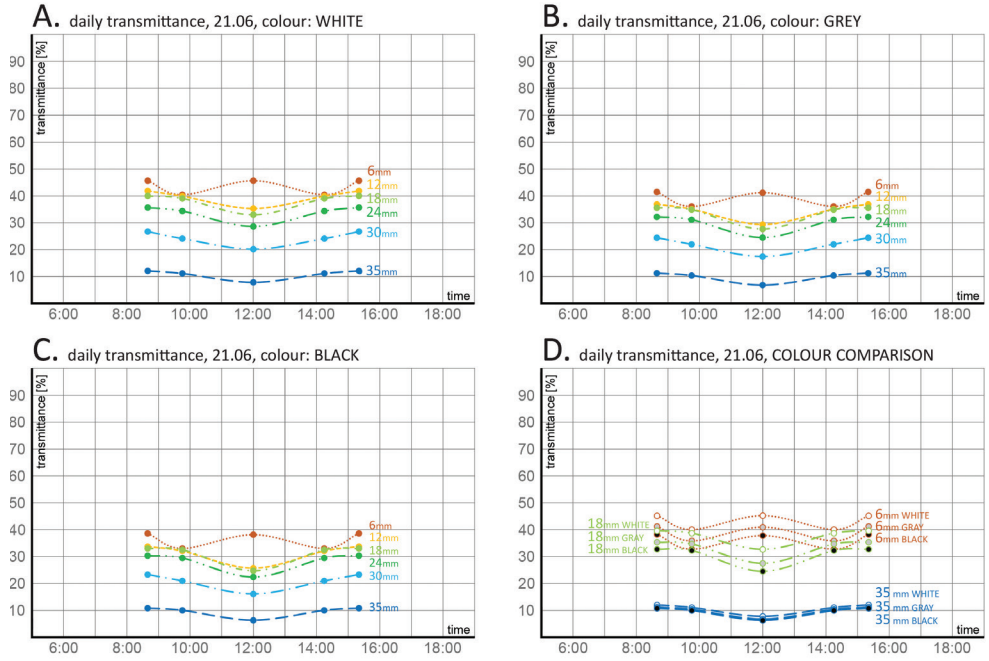

FIG. 15 Transmittance data through the day for the summer solstice (21st June). Each curve corresponds to a given strand-width, w (mm). The first three graphs correspond to each colour: white, grey, and black. The fourth graph shows the superposition of curves for the three colours and three strand-widths: 6, 24, and 35mm

Summer solstice means the highest sun angles and the longest day of the year but the shortest exposure of the southern façades. That is why the graphs (FIG 15) show quite a narrow daytime spectrum.

Besides, observing the Klems patch pattern obtained to fit the summer solstice sun path in Madrid (FIG 9.), it's evident that the sun path crosses very few patches. This is clearly one of the limitations of using the classic Klems dome method and it can be solved through the Tensor Tree method possibilities (De Michele et al., 2018).

EM meshes with strand width w=18 mm and higher seem to perform as expected, with the lowest transmittance values at midday. The flattening of the curves does not appear, but that might be due to a low number of control points.

In general, the upwards concavity remains with maximum values at dawn/dusk except for the 6 mm strand width mesh. This striking inversion of curvature can be explained by the shadow patterns of the mesh for corresponding lightning directions (FIG 16A). For the direction corresponding to the hour 9:45, see-through openings constitute below 15% of the overall mesh area, while for the angle at 12:00 they occupy over 31%.

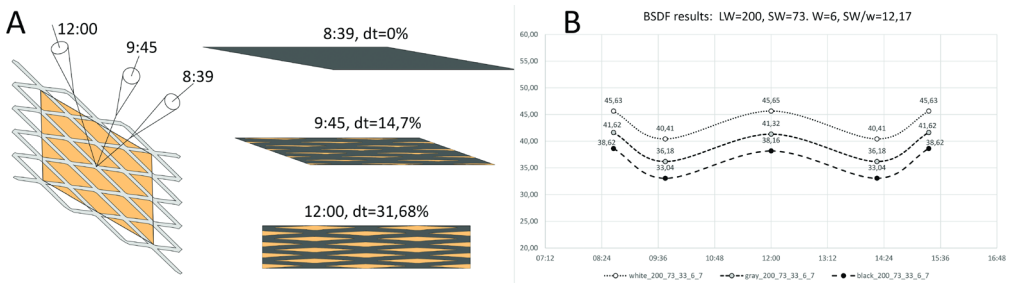

FIG. 16 [a] Shadow pattern analysis and transmittance analysis for the summer solstice (6mm strand width mesh) [b] Previously conducted lab results graph for a similar EM mesh, also showing maximum transmittance at midday.

In addition, a transmittance curve based on our physical lab measurements of a similar EM mesh seems to confirm that direct transmittance increases close to midday when it is normally expected to be at its lowest (FIG 16B)

The maximum transmittances, for white colour, were around 70%, with w=6mm in winter and 72% at the equinox. In summer, that maximum value drops to 46% due to the solar height.

The minimum values in summer are higher than in winter or the equinoxes.

The effect of the strand width is more noticeable on white coloured meshes than on black ones. For instance, at 10:00 and 14:00 the transmittance from w=6mm to w=35mm leaps 23 points on black, 27 points on grey and 30 points on white coloured meshes.

4.2 MIDDAY TRANSMITTANCE VALUES THROUGH THE YEAR BY STRAND WIDTH FOR SPECIFIC COLOURS

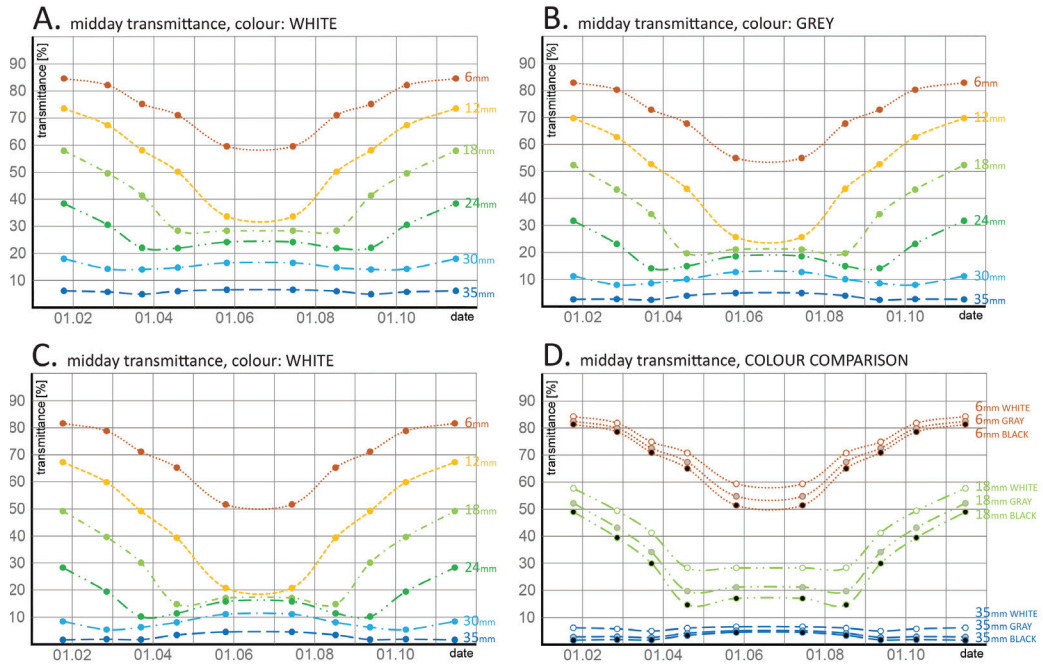

FIG. 17 Midday transmittance data throughout the year. Each curve corresponds to a given strand-width, w (mm). The first three graphs correspond to each colour: white, grey, and black. The fourth graph shows the superposition of curves for the three colours and three strand-widths: 6, 24, and 35mm

This set of graphs (FIG 17) analyses how the date of the year affects transmittance at midday (12:00).

As previously indicated (section 2.3.2), high values of opening ratio should involve bigger apertures and lead to higher transmittances and, consequently, the increase of strand width is inversely proportional to the transmittance.

The results shown here are coherent with this logic: on white meshes at the winter solstice one can observe transmittance values of 77% for w=6mm and 7% for w=35mm.

At the summer solstice, the transmittance differences drop because of the higher sun position, which reaches the façades tangentially and finds fewer openings for direct transmission.

Following the same logic, 35 mm strand width meshes show very few variations throughout the year, since their transmittance is very low.

The 6mm strand width mesh differs clearly from the rest at the summer solstice, with a transmittance nearly 25% higher than the following mesh. The transmittances of the rest of the meshes in summer show much smaller differences.

In winter, the increase of transmittance values is quite homogeneously proportional to the opening ratio.

For summer and lower opening ratios, midday-transmittances are actually higher than for winter. Similar data has been registered from lab assessment for meshes with low opening ratios as well (FIG 18). The hypothetical cause of this increase in transmittance in summer might be the additional transmission of incoming light after interior reflections on the surfaces of the mesh. The fact that darker colours of the mesh seem to amplify this trend seems to back it up.

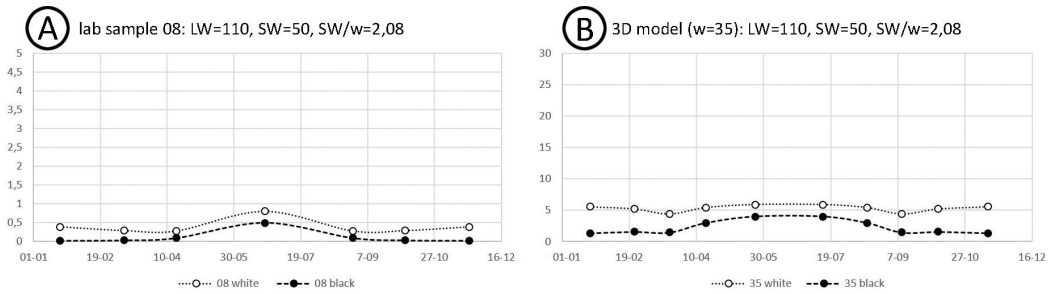

FIG. 18 Lab and BSDF results for EM meshes with similar proportions (Both meshes have an opening ratio of SW/w=2.08) [a] Lab results [b]. BSDF results

4.3 INFLUENCE OF STRAND WIDTH ON DAILY TRANSMITTANCE, BY TIMES OF THE DAY, FOR DIFFERENT DATES AND WHITE COLOUR

These curves (FIG 19) have been traced in order to directly show the relation between strand width and transmittance variation. Overall, it can be stated that the relation (the slope of the curves) is similar for different daytimes except for the dawn in the equinoxes.

Coherently, the amplitude of the curves is higher for the winter solstice with big transmittance differences for different strand widths. As seen before, these differences attenuate when passing to the equinoxes and reaching the summer.

Focusing on the winter solstice and excluding the dawn (7:21) data, simplified generalist statements like the following can be done: For a south-facing mesh located in Madrid, the variation of daylight transmittance is inversely proportional to the variation of strand width. That relation is practically linear with such a slope that an increase of 5 mm in strand width implies a decrease of around 12-15% of the transmittance.

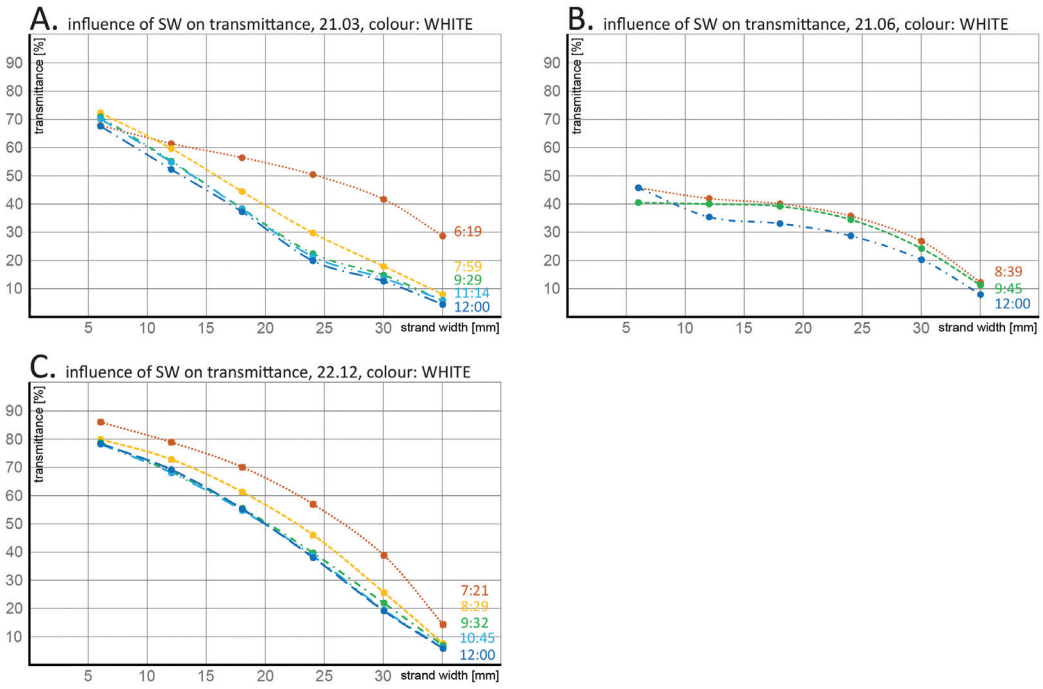

FIG. 19 Transmittance data versus EM strand width for white coloured meshes. Each curve corresponds to a given time of the day. The three graphs correspond to different dates: equinox, summer solstice, and winter solstice

4.4 INFLUENCE OF STRAND WIDTH ON MIDDAY TRANSMITTANCE, BY DATE FOR SPECIFIC COLOURS

In the same direction as that of the previous graphs, the midday transmittance - strand width relation has been expressed, but collecting in each graph the curves corresponding to several dates of the year (FIG 20).

It is noticed that, for the winter dates, the decline in transmittance as strand width increases is almost linear and with a similar slope until a certain value of the strand width. From w=24 mm, the curves show some curvature towards a horizontal asymptote that responds to the fact that it is getting close to zero transmittance. Nevertheless, moving away from winter, the curves show an increase of the slope (higher transmittance fall-offs for given strand width growths) and an inflection point. Getting closer to the summer, the inflection point moves to higher values of the strand width. A noticeably horizontal stretch is also observed where transmittance does not vary with the strand width. Those curves recover a certain slope to drop towards zero transmittance for high values of w (low values of the opening ratio).

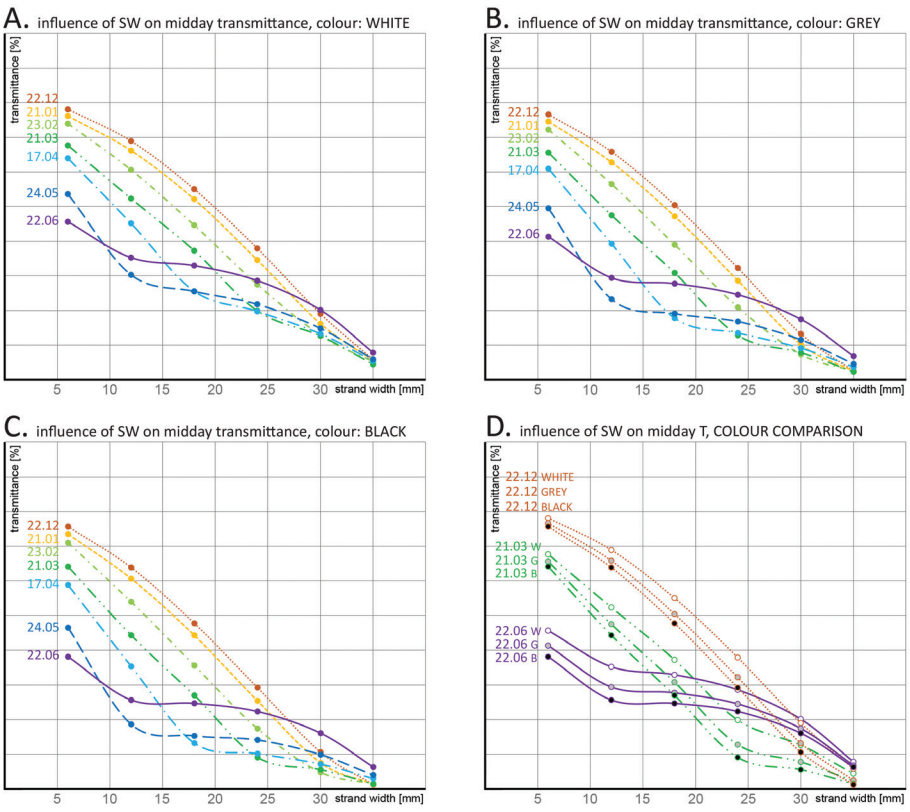

FIG. 20 Midday transmittance data versus EM strand width. Each curve corresponds to a given date. The three first graphs correspond to different colours: white, grey and black. The fourth graph shows the superposition of curves for the three colours and three dates: Winter solstice, equinox and summer solstice

4.5 INFLUENCE OF COLOUR ON TRANSMITTANCE

As could have been expected, the colour of the EM device affects the transmittance to a certain degree. The highest transmittance values were achieved for the white meshes and lowest for the black ones.

An overall difference of transmittance between black and white EM stayed between the range of 1.13% and 13.52%, with an average of 7.67%, which is notable. As seen in the comparison (TABLE 3), the overall influence of colour relies on the opening ratio and sun angles. One could attribute that reliance on the amount of light transmitted by interior reflections from the surface of the mesh, which varies due to the complex geometry of EM (FIG 21). Overall, for a given location, the influence of colour on transmittance seems to be the strongest for diamond shaped EM meshes with SW/w ratios between 0.25 and 0.33.

TABLE 3 Influence of colour on transmittance decrease (compared to white mesh)

DATE	22.06											
colour	grey						black					
time/w	6	12	18	24	30	35	6	12	18	24	30	35
8:39	4.01%	4.87%	4.29%	3.34%	2.23%	0.82%	7.01%	8.12%	6.95%	5.28%	3.42%	1.27%
9:45	4.24%	4.74%	4.07%	3.12%	2.06%	0.74%	7.38%	7.84%	6.53%	4.88%	3.17%	1.13%
12:00	4.33%	5.84%	5.22%	4.07%	2.70%	1.03%	7.49%	9.59%	8.26%	6.25%	4.05%	1.50%
14:15	4.24%	4.74%	4.07%	3.12%	2.06%	0.74%	7.38%	7.84%	6.53%	4.88%	3.17%	1.13%
15:21	4.01%	4.87%	4.29%	3.34%	2.23%	0.82%	7.01%	8.12%	6.95%	5.28%	3.42%	1.27%
average	4.16%	5.01%	4.39%	3.40%	2.26%	0.83%	7.25%	8.30%	7.04%	5.31%	3.44%	1.26%
summary	min	0.74%	max	5.84%	avg total	3.34%	min	1.13%	max	9.59%	avg total	5.43%

DATE	21.03											
colour	grey						black					
time/w	6	12	18	24	30	35	6	12	18	24	30	35
6:19	6.06%	7.63%	8.13%	7.34%	5.69%	4.84%	10.48%	13.04%	13.52%	11.88%	8.80%	6.85%
7:59	2.90%	5.07%	6.33%	6.53%	4.73%	2.09%	4.48%	7.84%	9.72%	9.83%	6.95%	2.98%
9:29	2.16%	4.51%	6.44%	6.80%	4.66%	2.08%	3.70%	7.48%	10.26%	10.39%	6.85%	2.90%
11:14	2.18%	4.60%	6.58%	7.18%	5.02%	2.21%	3.71%	7.53%	10.44%	10.92%	7.33%	3.06%
12:00	2.10%	4.85%	6.45%	7.09%	4.85%	2.14%	3.58%	8.04%	10.25%	10.78%	7.09%	2.98%
12:46	2.18%	4.60%	6.58%	7.18%	5.02%	2.21%	3.71%	7.53%	10.44%	10.92%	7.33%	3.06%
14:31	2.16%	4.51%	6.44%	6.80%	4.66%	2.08%	3.70%	7.48%	10.26%	10.39%	6.85%	2.90%
16:01	2.90%	5.07%	6.33%	6.53%	4.73%	2.09%	4.48%	7.84%	9.72%	9.83%	6.95%	2.98%
17:41	6.06%	7.63%	8.13%	7.34%	5.69%	4.84%	10.48%	13.04%	13.52%	11.88%	8.80%	6.85%
average	3.19%	5.38%	6.82%	6.98%	5.01%	2.73%	5.37%	8.87%	10.91%	10.76%	7.44%	3.84%
summary	min	2.08%	max	8.13%	avg total	5.02%	min	2.90%	max	13.52%	avg total	7.86%

DATE	22.12											
colour	grey						black					
time/w	6	12	18	24	30	35	6	12	18	24	30	35
7:21	1.92%	3.54%	4.80%	6.31%	6.65%	3.57%	2.58%	4.95%	6.67%	8.43%	8.64%	4.78%
8:29	1.61%	3.79%	5.42%	6.09%	5.43%	3.43%	2.51%	5.57%	7.82%	8.72%	7.80%	4.68%
9:32	1.61%	3.37%	4.82%	5.56%	5.56%	3.45%	2.58%	5.38%	7.50%	8.42%	8.04%	4.69%
10:45	1.47%	3.20%	4.70%	5.62%	5.61%	3.19%	2.43%	5.25%	7.42%	8.54%	8.12%	4.34%
12:00	1.48%	3.11%	4.61%	5.68%	5.85%	3.36%	2.43%	5.06%	7.32%	8.67%	8.43%	4.56%
13:15	1.47%	3.20%	4.70%	5.62%	5.61%	3.19%	2.43%	5.25%	7.42%	8.54%	8.12%	4.34%
14:28	1.61%	3.37%	4.82%	5.56%	5.56%	3.45%	2.58%	5.38%	7.50%	8.42%	8.04%	4.69%
15:31	1.61%	3.79%	5.42%	6.09%	5.43%	3.43%	2.51%	5.57%	7.82%	8.72%	7.80%	4.68%
16:39	1.92%	3.54%	4.80%	6.31%	6.65%	3.57%	2.58%	4.95%	6.67%	8.43%	8.64%	4.78%
average	1.63%	3.44%	4.90%	5.87%	5.82%	3.41%	2.52%	5.26%	7.35%	8.54%	8.18%	4.61%
summary	min	1.47%	max	6.65%	avg total	4.18%	min	2.43%	max	8.72%	avg total	6.08%

DATE	YEAR AVERAGE (AT NOON)											
colour	grey						black					
w	6	12	18	24	30	35	6	12	18	24	30	35
average	2.90%	4.78%	5.90%	6.11%	4.80%	2.62%	4.86%	7.77%	9.30%	9.28%	7.02%	3.65%
summary	min	0.74%	max	8.13%	avg total	4.52%	min	1.13%	max	13.52%	avg total	6.98%

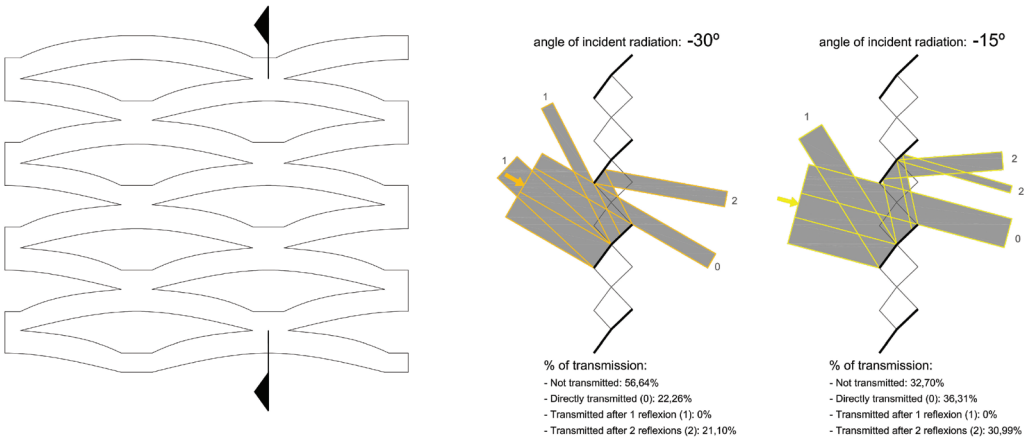

FIG. 21 Examples of simplified interior reflections (considering specular reflectance)

5 CONCLUSIONS

5.1 PARAMETERS AFFECTING TRANSMITTANCE - SUMMARY

The parameters affecting transmittance are divided into three general groups:

- EM mesh geometry: shape and proportions
- Incoming light direction (in relation to mesh face): sun azimuth (longitude) and solar height (latitude)
- EM mesh colour

To assess real-life situations it is necessary to refer the light direction to mesh localisation and position, time, and date. Overall, the impact of each parameter on transmittance depends on other parameters. As seen, transmittance depends on both mesh geometry and sun angle; it must be considered to what extent the decrease of the opening ratio (SW/w) of Expanded Metal meshes results in lower transmittances for given solar heights.

Mesh proportions - The most significant factor in terms of mesh geometry is definitely the opening ratio (SW/w), although, as seen in the results, this is not a linear, easy-to-describe general correlation between the opening ratio and daylight transmittance. The change of strand width also influences other proportions. It is worth remembering, those other parameters can also strongly influence the mesh geometry, affecting the shading performance. The complex geometry of the EM also makes its shading performance less predictable in terms of light direction.

In general, greater transmittance increases have been observed due to the variation of strand width of EM meshes at the winter solstice (70 to 75 percent points from w=35 to w=6 mm).

As stated in section 4.3, on the winter solstice, for most times of day, a south-facing mesh in Madrid presents a nearly linear variation of daylight-transmittance inversely proportional to the variation of strand width; an increase of 5 mm in strand width implies a decrease of around 12-15% of the transmittance.

It is worth mentioning that low values of the opening ratio lead to meshes that almost totally prevent direct vision through them. This is a very limiting condition for an element to be included in a complex fenestration system.

Solar Height

This is the most obvious and one of the most important factors affecting the transmittance values. As a rule, the higher the position of the sun, the lower the transmittance. However, as seen on the graphs that show transmittance throughout the year (section 4.2), the relationship is not linear and once the solar height and SW/w ratio are high enough, an inversion of the curvature may occur.

Solar height is related to the season, of course.

The maximum transmittances, for white colour, were around 70% with w=6mm in winter and 72% at the equinox. In summer, that maximum value drops to 46% of the solar height.

The minimum values in summer are higher than in winter or the equinoxes. Minimum summer transmittance with black colour is around 7%, while at the equinox it drops to 2% and in winter to 1%. These values always appear at midday.

Sun Azimuth

Similarly to the solar height, the transmittance is at its maximum when the sun azimuth is perpendicular to the mesh plane and decreases as it moves towards the mesh plane. Although, in general, solar height seems to be slightly more influential on the transmittance, overall sun direction is always a sum of both latitude and longitude. This sometimes leads to counterintuitive outcomes, such as the temporary rise of transmittance towards midday, as seen for the summer solstice in FIG 15.

Colour

Colour influences the indirect transmittance (transmittance through internal reflection). Therefore, the influence of colour relies on SW/w and the direction of incoming light. As expected, darker colours led to a decrease of transmittance.

5.2 GENERAL ASPECTS FOR FAÇADE DESIGNERS.

5.2.1 Position and tilt of the building envelope

The data shown in this paper relates to an envelope facing directly south, and perpendicular to the ground. Change of either orientation or tilt of the EM's surface obviously changes the relative sun angles, strongly affecting the performance. Therefore, it is essential to consider each aspect. In general, an upwards tilt of the envelope usually causes an increase of transmittance while a downward tilt decreases it. A change of orientation for the façade changes the timeslot in which the direct sunlight reaches it, which, of course, also affects the performance.

5.2.2 The necessity of detailed research and on purpose simulation

Due to the multiple variable conditions of the issue it is not possible to state strictly linear relations between any particular parameter (or group of parameters) and the shading performance of EM. While most assumptions about the influence of those parameters are correct, they are too general to reliably predict the real-life performance. For proper assessment, it is necessary to run a specific simulation, which takes into account the specific mesh model and colour, as well as its position and location.

5.2.3 Presence of shadow patterns

Due to the visible shading patterns, EM meshes are generally not suitable for any spaces in which precision work is done, such as labs, workshops, or offices. For such spaces, it is recommended to use either fine (densely distributed, small openings) EM meshes, or an additional layer of diffuse material.

5.2.4 The complexity of façade systems

It is worth remembering that EM meshes are usually just a part of a façade/fenestration system, with its different layers working as a whole. Therefore, to analyse the whole behaviour it is necessary to include all layers and elements of the façade. Furthermore, to obtain real-life performance it is also crucial to take into account the environmental data, such as the intensity of light, or amount of incoming diffused light. Only then can the illumination of the building's interior and solar energy gains be closely predicted and balanced.

5.3 OBSERVATIONS ON BSDF DATA FOR REAL LIFE DAYLIGHT TRANSMITTANCE ASSESSMENT.

5.3.1 Potential usage

Thanks to previously conducted lab measurements (Rico-Martinez, 2015), statements that one could intuitively predict, without analysis, were proved valid and expressed measurably.

In particular, the ratio SW/w appeared as a depictive feature of EM meshes. However, they have also shown that it is difficult to predict and summarise transmittance behaviour for EM and one cannot relate it simply and directly to geometrical mesh features such as SW/w ratio or the surface of the openings. Therefore, to predict the EM performance more closely it is necessary to consider tools that take into account multiple factors such as specific geometry and outside finish of mesh or specific directions of incoming light. One of the advantages is that, once the simulation for a particular EM shading is done and saved, it provides a large database, allowing the device shading performance to be simulated for every possible position or location. Such data can also be part of more in-depth analysis, considering the complete complex fenestration and façades systems, diffused light transmittance, and the influence of other environmental factors to allow for detailed and accurate performance analysis. Even as is, the data can be useful for designers needing to choose adequate EM shading systems.

5.3.2 Usage of classic Klems dome as a source of inaccuracies

In the classic Klems pattern, each patch represents a range of directions and transmittance values are calculated for the sum of those directions. Decreasing the size of the patches as with Tensor tree BSDF (Ward, Kurt, & Bonneel, 2012) would also reduce the inaccuracies (the lower the patch, the more accurate the results). Another option could be to use custom ray-tracing simulations for particular directions.

Acknowledgments

We want hereby to acknowledge:

- The support of the Environment, Territorial Planning and Housing of the Basque Government.
- The support of the Architecture Department of the University of the Basque Country
- The advice of Xavier Ferrés (Doctor Architect – Façade Consultant), Zigor Marroquin (Façade Engineer) and Patxi Rubín (Engineer - Technical Director of Industrias Imar S.A.).

In this paper, the SDC (sequence-determines-credit) approach for the authors order has been followed.

References

Alatawneh, B.M.K., Nobile, M.R., Germanà, M.L., & Reffat, R.M. (2016). *THE PERFORATED BUILDING'S ENVELOPE: GUIDING THE EARLY DESIGN PHASES*. 317.

Begemann, S. H. A., van den Beld, G. J., & Tenner, A. D. (1997). Daylight, Artificial Light and People in an Office Environment, Overview of Visual and Biological Responses. *International Journal of Industrial Ergonomics* 20(3):231–39.

Brzezicki, M. (2012). The influence of reflected solar glare caused by the glass cladding of a building: application of caustic curve analysis. *Computer-Aided Civil and Infrastructure Engineering*, *27*(5), 347-357.

Curic Studio. n.d. 'Curic Sun | SketchUp Extension Warehouse'. Retrieved 21 May 2020 (https://extensions.sketchup.com/extension/49b56362-ada6-4bde-8213-8c68eb7763d1/curic-sun).

De Michele, G., Loonen, R., Saini, H., Favoino, F., Avesani, S., Papaiz, L., & Gasparella, A. (2018). Opportunities and challenges for performance prediction of dynamic Complex Fenestration Systems (CFS). *Journal of Façade Design and Engineering*, *6*(3), 101-115.

Fernandes, L. L., Lee, E.S., McNeil, A., Jonsson, J.C., Nouidui, T., Pang, X., & Hoffmann, S. (2015). Angular Selective Window Systems: Assessment of Technical Potential for Energy Savings. *Energy and Buildings* 90:188–206.

Klems, J. H. (1994). New Method for Predicting the Solar Heat Gain of Complex Fenestration Systems- 2. Detailed Description of the Matrix Layer Calculation. *ASHRAE Transactions* 100(1):1073–1086.

Littlefair, P. (2001). Daylight, Sunlight and Solar Gain in the Urban Environment. *Solar Energy* 70(3):177–85.

Loonen, R.C.G.M, Rico-Martinez, J. M., Favoino, F., Brzezicki, M., Menezo, C., La Ferla, G., & Aelenei, L. (2015). Design for Façade Adaptability–Towards a Unified and Systematic Characterization. Pp. 1274–84 in *Proc. 10th Energy Forum-Advanced Building Skins, Bern, Switzerland*.

McNeil, A., Jonsson, C. J., Appelfeld, D., Ward, G., & Lee, E. S. (2013). A Validation of a Ray-Tracing Tool Used to Generate Bi-Directional Scattering Distribution Functions for Complex Fenestration Systems. *Solar Energy* 98:404–14.

McNeil, A., Jonsson, J., & Appelfeld, D. (2011). *Validation of GenBSDF. 10th International Radiance Workshop*.

Michele, De., G., Loonen, R., Saini, H., Favoino, F., Avesani, S., Papaiz, L., & Gasparella, A. (2018). Opportunities and Challenges for Performance Prediction of Dynamic Complex Fenestration Systems (CFS)'. *Journal of Facade Design and Engineering* 6(3):101–15.

Nicodemus, F. E. (1965). 'Directional Reflectance and Emissivity of an Opaque Surface'. *Applied Optics* 4(7):767–773.

Perry, M. J. (1990). Mechanisms of Discomfort Glare. *Lighting Research & Technology* 22(3):159–159.

Rico-Martinez, J. M. (2015). *Methods and Tools for the Assessment of Daylight Transmittance through Expanded Metal Meshes*. University of the Basque Country, Donostia-San Sebastian.

Robbins, C. L. (1985). Daylighting. Design and Analysis.

Sadeghipour Roudsari, Mostapha. (n.d). 'Ladybug Tools | Ladybug'. *Ladybug*. Retrieved 21 May 2020 https://www.ladybug.tools/ladybug.html.

Saini, H., Loonen, R. C. G. M, & Hensen, J.L.M. (2018). Simulation-Based Performance Prediction of an Energy-Harvesting Facade System with Selective Daylight Transmission. Pp. 213–19 in *VIII International Congress on Architectural Envelopes*.

Ward, G., Mistrick, R., Lee, E. S., McNeil, A., & Jonsson, J. (2011). Simulating the Daylight Performance of Complex Fenestration Systems Using Bidirectional Scattering Distribution Functions within Radiance. *LEUKOS* 7(4):241–61.

Ward, G., Kurt, M., & Bonneel, N. (2012). *A Practical Framework for Sharing and Rendering Real-World Bidirectional Scattering Distribution Functions*. LBNL--5954E, 1172245.